Connectivity-based parcellation reveals distinct cortico-striatal connectivity fingerprints in Autism Spectrum Disorder

Author(s):
Balsters, Joshua H.; Mantini, Dante; Wenderoth, Nicole

Publication date:
2018-04-15

Permanent link:
https://doi.org/10.3929/ethz-b-000129137

Originally published in:
NeuroImage 170, https://doi.org/10.1016/j.neuroimage.2017.02.019

Funding acknowledgement:
ETH-38 16-2 - Linking meso- and macro-scale cortico-striatal functional connectomics: a DREADD-rsFMRI approach (ETHZ)

NeuroImage 170 (2018) 412–423

Contents lists available at ScienceDirect

NeuroImage

journal homepage: www.elsevier.com/locate/neuroimage

Connectivity-based parcellation reveals distinct cortico-striatal connectivity fingerprints in Autism Spectrum Disorder

Joshua H. Balsters[a,b,*], Dante Mantini[a,c,d], Nicole Wenderoth[a,d]

[a] Neural Control of Movement Laboratory, Department of Health Sciences and Technology, ETH Zurich, Switzerland
[b] Department of Psychology, Royal Holloway University of London, Egham, Surrey, UK
[c] Department of Experimental Psychology, University of Oxford, Oxford OX1 3UD, UK
[d] KU Leuven, Kinesiology and Rehabilitation Sciences, Research Center for Movement Control and Neuroplasticity, Heverlee, Belgium

ARTICLE INFO

Keywords:
Autism Spectrum Disorder
Basal ganglia
Connectivity-based parcellation
Resting state fMRI

ABSTRACT

Autism Spectrum Disorder (ASD) has been associated with abnormal synaptic development causing a breakdown in functional connectivity. However, when measured at the macro scale using resting state fMRI, these alterations are subtle and often difficult to detect due to the large heterogeneity of the pathology. Recently, we outlined a novel approach for generating robust biomarkers of resting state functional magnetic resonance imaging (RS-fMRI) using connectivity based parcellation of gross morphological structures to improve single-subject reproducibility and generate more robust connectivity fingerprints. Here we apply this novel approach to investigating the organization and connectivity strength of the cortico-striatal system in a large sample of ASD individuals and typically developed (TD) controls (N=130 per group). Our results showed differences in the parcellation of the striatum in ASD. Specifically, the putamen was found to be one single structure in ASD, whereas this was split into anterior and posterior segments in an age, IQ, and head movement matched TD group. An analysis of the connectivity fingerprints revealed that the group differences in clustering were driven by differential connectivity between striatum and the supplementary motor area, posterior cingulate cortex, and posterior insula. Our approach for analysing RS-fMRI in clinical populations has provided clear evidence that cortico-striatal circuits are organized differently in ASD. Based on previous task-based segmentations of the striatum, we believe that the anterior putamen cluster present in TD, but not in ASD, likely contributes to social and language processes.

Introduction

For over a century, neuroanatomists have parcellated the human brain based on its *intrinsic properties* such as cyto- and myeloarchitecture (Amunts and Zilles, 2015). These parcellations are often based on a small number of postmortem brains (typically 1–10), and thus it is not clear to what extent they are representative of the general population. Small sample sizes mean that it is also impossible to say whether variations in the parcellation of individuals with psychiatric conditions reflects inter-individual variability or whether these differences are a feature of the pathology. Novel tools such as resting state (RS) fMRI are now increasingly employed to partition gross morphological regions into functional sub-units based on *extrinsic connectivity* patterns (a procedure often referred to as connectivity-based parcellation; Eickhoff et al., 2015; Gordon et al., 2014; Wig et al., 2014; Yeo et al., 2011). Whilst brain parcellation using RS-fMRI is predominantly based on extrinsic connectivity patterns, other metrics are increasingly being explored such as Graph theory (Shen et al., 2010, 2013), infinite Gaussian mixture models (Janssen et al., 2015), and von Mises-Fisher distributions and Markov random fields (Ryali et al., 2013). The growth of freely available RS-fMRI databases such as the Autism Brain Imaging Data Exchange (ABIDE: Di Martino et al., 2014b), in combination with increasingly sophisticated signal processing methods, have allowed researchers to address previously unanswerable questions regarding the organisation and structure of brain circuits in psychiatric disorders. Here, we will employ recently published connectivity-based parcellation methods (Balsters et al., 2016) to investigate differences in the organisation of cortico-striatal circuitry in Autism Spectrum Disorder (ASD).

The seminal work of Alexander et al. (1986) first demonstrated that distinct regions of the frontal lobe project to distinct regions of the striatum. The dominant projections to the caudate nucleus originate in regions of the prefrontal cortex concerned with cognitive control such as the dorsolateral prefrontal cortex, lateral portions of the orbito-

* Corresponding author at: Neural Control of Movement Laboratory, Department of Health Sciences and Technology, ETH Zurich, Switzerland.
E-mail address: Joshua.balsters@hest.ethz.ch (J.H. Balsters).

http://dx.doi.org/10.1016/j.neuroimage.2017.02.019
Received 13 December 2016; Accepted 7 February 2017
Available online 08 February 2017

frontal cortex, and oculomotor regions. The nucleus accumbens (NAcc) receives projections from limbic regions linked to reward processing and value-based decision making such as the anterior cingulate cortex, orbitofrontal and ventromedial prefrontal cortex. Finally, the putamen receives projections from regions concerned with action planning and motor control such as the premotor and primary motor cortex, as well as somatosensory regions. This fundamental cortico-striatal organisation has not only been demonstrated in nonhuman primates (Middleton and Strick, 2000; Selemon and Goldman Rakic, 1985; Yeterian and Pandya, 1991), but also through non-invasive methods in humans such as diffusion imaging (Draganski et al., 2008; Tziortzi et al., 2014; Verstynen et al., 2012) and RS-fMRI (Choi et al., 2012; Janssen et al., 2015; Jaspers et al., 2016; Jung et al., 2014). Although most studies agree that the cortico-striatal system mirrors the rostral-caudal organisation of the frontal lobe, the optimal parcellation of the striatum is still a debated issue. Previous RS-fMRI studies parcellating the human striatum have suggested that the caudate nucleus can be segmented into 1–9 functionally unique sub-units, whilst the putamen can be segmented into 1–6 clusters (Choi et al., 2012; Janssen et al., 2015; Jaspers et al., 2016; Jung et al., 2014). While most previous striatal parcellations have been based on task-independent data, a recent study by Pauli et al. (2016) used task-dependent meta-analytic data to segment the striatum into five regions. These five segments of the striatum were associated with unique behaviours, specifically: incentive behaviour (anterior caudate), executive functions (posterior caudate), social and language processes (anterior putamen), sensorimotor processes (posterior putamen), and stimulus value (ventral striatum/NAcc). Although there is still some debate surrounding the correct number of distinct cortico-striatal circuits, it is certainly clear that the human striatum contributes to a combination of cognitive, social, motor, and motivational processes (see meta-analyses: Pauli et al., 2016; Robinson et al., 2012), all of which are known to be affected in ASD (Chevallier et al., 2012; Dichter and Adolphs, 2012; Fuccillo, 2016; Kohls et al., 2014b).

Several studies have proposed that abnormalities in cortico-striatal circuitry could underlie the two core deficits in ASD: 1) social interaction and communication difficulties and 2) restricted interests and repetitive behaviours. A large number of studies have shown increased striatal volume in individuals with ASD (Haznedar et al., 2006; Hollander et al., 2005; Langen et al., 2009) and differences in striatal shape (Schuetze et al., 2016). Langen et al. (2009, 2013) showed that striatal volume increased with age in individuals with ASD, whilst it appeared to decrease with age in typically developing (TD) individuals, and the rate of striatal growth in ASD correlated with the severity of restrictive and repetitive behaviours. Hollander et al. (2005) similarly showed that increased striatal volume was correlated with increased restricted and repetitive behaviour in ASD. RS-fMRI studies have also consistently demonstrated greater cortico-striatal functional connectivity in ASD compared to TD (Cerliani et al., 2015; Delmonte et al., 2013; Di Martino et al., 2011; Padmanabhan et al., 2013). In addition, both Padmanabhan et al. (2013) and Cerliani et al. (2015) showed distinct cortico-striatal developmental trajectories in ASD compared to TD individuals. However, Padmanabhan et al. (2013) showed cortico-striatal connectivity decreasing with age in ASD, whilst Cerliani et al. (2015) found cortico-striatal connectivity decreased with age in TD and did not change with age in ASD. Both Delmonte et al. (2013) and Cerliani et al. (2015) also showed that the extent to which cortico-striatal circuits were hypoactive correlated with both social and communication deficits as well as restricted and repetitive behaviours. Lastly, a number of studies using cognitive and sensorimotor paradigms have shown aberrant striatal activity in ASD (Schmitz et al., 2006; Scott-Van Zeeland et al., 2010b; Takarae et al., 2007). In addition to cognitive and motor paradigms, the social incentive delay task (Rademacher et al., 2010) has also been used extensively to highlight aberrant striatal BOLD responses in ASD during the anticipation and receipt of social rewards (Delmonte et al., 2012; Kohls et al., 2014a; Scott-Van Zeeland et al., 2010a). Delmonte et al. (2013) used RS-fMRI collected from the same ASD individuals that previously performed a social incentive delay task (Delmonte et al., 2012) to show that cortico-striatal resting connectivity strength was correlated with striatal BOLD responses to social rewards.

There is largely consistent evidence to suggest that aberrant cortico-striatal connectivity may be a feature of ASD pathology, however, studies of inter-individual differences such as changes in RS-fMRI connectivity with age have provided inconsistent results. In addition, no study to date has investigated whether the organisation of cortico-striatal circuits is more variable in ASD compared to TD (Hahamy et al., 2015) or whether cortico-striatal circuits are missing altogether in ASD. These questions can be addressed using the connectivity-based parcellation methods outlined in Balsters et al. (2016). Balsters et al. (2016) demonstrated that seeds generated using connectivity-based parcellation significantly improved resting state network detection, and as such connectivity-based parcellation could reduce inconsistencies seen in previous ASD ageing studies. The cortico-striatal system is also an excellent model for connectivity-based parcellation given that so much is known about its organisation from animal tracer studies and human neuroimaging. This provides an excellent reference with which to compare cortico-striatal circuitry in ASD. Using methodologies described in Balsters et al. (2016) we will use a large RS-fMRI dataset (N=260, 50% ASD) to investigate whether the parcellation of the striatum, and cortico-striatal connectivity, is different in ASD compared to TD.

Methods

Participants

Data were extracted from the ABIDE database (Di Martino et al., 2014b) using the same exclusion criteria as Di Martino et al., (2014b). Subjects were excluded if they were: female, > 40 yrs old, IQ < 80, or moved excessively (mean framewise displacement (FD) > 0.5 mm). It was important to remove these individuals as they were not well represented in the ABIDE database and their inclusion in the analyses would introduce additional variability or a potential bias. Given our interest in developmental trajectories we excluded a small number of older individuals (> 40 yrs old) who all came from one centre and might artificially drive age effects or Group×age interactions. We additionally removed subjects with poor gray matter (GM) segmentation as this would impact on DARTEL template quality and subsequent normalisation. GM segmentation was assessed using the squared distance of each image to the sample mean (tool available in the VBM8 toolbox: http://dbm.neuro.uni-jena.de/vbm/download). If this distance was > 2 SD from the sample mean from the same scanning centre then the subject was removed. Datasets were also excluded if they did not have whole brain coverage (signal present at z=−55 (ventral bound of Crus II) or lower after normalisation). This lead to 11/28 centres (500 datasets) being excluded. A centre was also rejected if it had < 7 ASD or TD individuals that met our inclusion criteria. After rejection, nine centres contributed to this study with 131 ASD and 169 TD datasets. We subsequently matched the two groups for age, full scale IQ, and head movement. This left 130 ASD and TD individuals in each group. Group demographics are reported in Table 1 showing the matching between groups in age, IQ, and head movement (FD and the number of bad volumes removed during scrubbing).

Pre-Processing

Initial pre-processing was conducted in SPM12 (www.fil.ion.ucl.ac.uk/spm). Structural Images were first coregistered to the T1 template before the New Segmentation toolbox was used to segment the data into GM, white matter (WM), and cerebro spinal fluid (CSF) images

Table 1
Participant demographics.

	TD				ASD					
	Min	Max	Mean	SD	Min	Max	Mean	SD	t value	p value
Age (yrs)	7.26	31.78	14.87	4.90	7.15	32.00	13.94	4.30	1.62	0.11
IQ	83.00	135.00	109.40	11.55	81.00	136.00	106.82	12.86	1.70	0.09
Framewise Displacement (mm)	0.08	0.31	0.17	0.05	0.06	0.28	0.17	0.05	0.07	0.95
Number of bad volumes (%)	**0**	**34.21**	**7.41**	**8.22**	**0**	**39.73**	**8.38**	**8.43**	**0.94**	**0.35**

ready for input to the DARTEL toolbox (Ashburner, 2007). The DARTEL toolbox was used to create a study specific template given that the average age of participants was 14yrs ± 4yrs, and as such the MNI template (generated using 18–30 yrs old brains) would not be appropriate (Wilke et al., 2008). Functional images were coregistered to the individual structural images, realigned, normalized to DARTEL template space (resliced to 3×3×3 mm), and smoothed with an 8mm kernel. All analyses were conducted in DARTEL template space and the final results were warped into MNI space for generating figures and anatomical localization guided by the Anatomy toolbox (Eickhoff et al., 2006, 2007, 2005), the Harvard-Oxford cortical and subcortical atlases, and FSL connectivity atlases (Mars et al., 2011, 2012; Neubert et al., 2015, 2014; Sallet et al., 2013).

Further data pre-processing was conducted using in-house scripts written using MATLAB (MathWorks, Natwick, MA). The first 4 volumes were discarded for steady state magnetization and stabilization of participant status. Data were 'scrubbed' to remove bad datapoints (> 0.5 mm FD or > 0.5% differential spatial variance - DVARS; Power et al., 2012), and filtered in the band 0.01–0.15 Hz. Typically, resting state studies ignore oscillations > 0.1 Hz, however, studies by Baria et al., (2011), and Balsters et al. (2013) have demonstrated that signals between 0.1–0.2 Hz contain physiologically relevant information that can often be used to distinguish between clinical populations. Adequately correcting for head motion artifact has proven to be an essential step in RS-fMRI analyses, especially in investigations of ASD (Deen and Pelphrey, 2012; Tyszka et al., 2014). Based on Yan et al., (2013), and Satterthwaite et al., (2013), we modeled head movement using the Friston 24-parameter approach (Friston et al., 1996) to remove potential residual head motion signal (6 original regressors generated during realignment, 6 time shifted regressors, and both of these squared) along with the first 5 principle component time series extracted from individual WM and CSF masks (Chai et al., 2012). Pruim et al. (2015a) showed that spike-regression, scrubbing, and ICA-based methods were the best approaches for dealing with movement artefacts. However, spike-regression and scrubbing also significantly reduce the temporal degrees of freedom and can reduce the integrity of the temporal data. The number of bad volumes removed in ASD and TD were not significantly different from each other (see Table 1) indicating that there should not be any group differences in the temporal degrees of freedom, however, in the future we hope to implement automatic approaches such as ICA-AROMA (Pruim et al., 2015b) or wavelet despiking (Patel et al., 2014) that might help to improve the temporal integrity of RS-fMRI data.

Hierarchical clustering

In order to partition the striatum into subregions with unique connectivity fingerprints we began by creating a mask using the Harvard-Oxford subcortical atlas. Masks of the caudate nucleus, nucleus accumbens, and putamen were thresholded at > 25% and summed to create a mask of the striatum. This mask was separated into the left and right striatum and then warped into DARTEL space. To establish connectivity fingerprints for each subject we extracted the RS-fMRI time-courses of the voxels belonging to the left or right striatum mask and those belonging to all left or right GM voxels in the brain (including the original striatum mask). All these analyses were restricted to either the left or right hemisphere given that cortico-striatal loops are known to be hemisphere specific (Alexander et al., 1986). We then calculated the correlation matrix between these two sets of time-courses, and transformed it to z-values using the Fisher r-to-z transformation. Each column of this correlation matrix reflected the connectivity of a voxel within the striatum mask with all GM voxels within the same hemisphere. We then performed a fixed-effects analysis of the matrices separately for the ASD and TD groups. The resulting matrix was transformed back to correlation values using the inverse Fisher transformation and used as input to a hierarchical clustering algorithm (average linkage). The resulting dendrogram was cut to identify cluster solutions ranging from 2 to 20. In order to determine which clustering solution was most appropriate we used the silhouette measure (Rousseeuw, 1987) to quantify to what extent the results derived from the group corresponded to individual data. The silhouette value assesses cluster separation by measuring how similar a voxel is to other voxels in the same cluster compared to voxels in the nearest cluster, thus maximizing within cluster similarity and between cluster differences. A silhouette value was generated for each cluster solution and for each individual subject, and a paired t-test (10,000 permutations) was used to determine where clustering solutions showed a significant improvement from one clustering solution to the next (i.e. is the silhouette value for a two cluster solution significantly larger (and therefore more representative across individuals) compared to a three cluster solution?). This was repeated comparing the silhouette value for a three cluster solution to the silhouette value for a four cluster solution, a four cluster solution to a five cluster solution etc. The voxels belonging to a given cluster were mapped back in the brain space to generate seeds to be used in further analyses. Single-subject clustering solutions were generated by running the same hierarchical clustering procedure on individual correlation matrices and cutting the dendrogram at a position equaling the number of clusters provided by the previous group-level estimates. Finally, we used the Dice similarity measure (Dice, 1945) to compare the entire set of group-level clusters (i.e. 5 clusters) to the clusters derived for an individual (also 5 clusters) (see Balsters et al. (2016) and Mantini et al. (2013) for further details). The matrix of Dice similarity values (i.e. spatial overlap between every group-level cluster and every individual-level cluster) was input into a hierarchical clustering algorithm (average linkage). After the creation of the dendrogram, we selected the cutoff value for the graph that yielded the maximum number of two-element clusters (i.e. a match between one group-level and one individual cluster). Note that this method does not enforce a minimal overlap cutoff value between a group cluster and the individual cluster solution but rather provides an optimal match across all clusters.

Seed-to-Voxel analyses

Seeds generated through hierarchical clustering were used to establish seed-to-voxel connectivity fingerprints and subsequently group differences in connectivity. First, a timecourse was extracted for each seed region (averaged across voxels within the seed) and this timecourse was correlated with all left or right hemisphere GM voxels in the brain. As previously mentioned, analyses were restricted to

either the left or right hemisphere given that cortico-striatal loops are known to be hemisphere specific (Alexander et al., 1986). Individual correlation maps were Fisher r-to-z transformed and fed into a General Linear Model (GLM) with 10,000 permutations in Randomise (http://fsl.fmrib.ox.ac.uk/fsl/fslwiki/; (Jenkinson et al., 2012; Winkler et al., 2014)). The GLM included scanning centre, mean FD, Full scale IQ, Group, age (log transformed to account for skewed distribution), and Group×age interaction. To correct for multiple comparisons at the cluster-level, we employed Gaussian random field theory, voxel-level Z > 3.1, cluster-level $p < 0.05$ FWE, based on Woo et al. (2014).

Multivariate comparisons of connectivity fingerprints

As well as using a traditional mass univariate approach to compare cortico-striatal connectivity in ASD and TD, we used the MR Comparative Analysis Toolbox (Mr Cat, www.neuroecologylab.org) to compare connectivity fingerprints as described in Mars et al. (2016). We began by defining our connectivity fingerprints as regions (targets) showing significant connectivity with the anterior or posterior putamen cluster, i.e. peaks of the seed-to-voxel analysis that survived thresholding at $p < 0.001$ uncorrected. After establishing our targets we extracted the seed-to-target connectivity strength (average Z value) for all target regions using a 6mm radius sphere around the peak co-ordinate (co-ordinates provided in Supplemental Table 1). We then calculated the Manhattan distance between connectivity fingerprints to determine whether connectivity fingerprints were significantly different from one another. This was done within group to establish whether different striatal clusters produced unique connectivity fingerprints, and between groups to determine whether connectivity fingerprints were different in ASD and TD. Significance was established using permutation testing (10,000 permutations) to create a test distribution. If there was a significant difference between connectivity fingerprints, we used logistic regression to establish which target regions were driving the differences.

Results

Group differences in connectivity-based parcellation of the striatum

We began by enforcing connectivity-based parcellation solutions separately for the left and right striatum ranging from 2 to 20 clusters. As in previous studies (Balsters et al., 2016; Jaspers et al., 2016; Pauli et al., 2016), we found that simpler solutions (i.e. fewer clusters) had the highest silhouette value in both hemispheres of ASD and TD individuals (Fig. 1a and Supplemental Fig. 1). Significant improvements in the clustering of the left striatum in the TD group (i.e. significantly larger silhouette value) were found for 2, 3, 5–9, 15, and 17 clustering solutions (blue dots in Fig. 1a), whilst the left striatum in ASD showed significant increase in silhouette value at 2–4, 6, 9–11, 14, 15, 17, and 18 cluster solutions (green dots in Fig. 1a). When comparing solutions between groups it was clear that ASD and TD clustering solutions deviated at the five cluster solution of the left striatum (Fig. 1a black asterisk). Whilst the five cluster solution was another significant improvement in the clustering solution of the TD group, partitioning the left striatum into five clusters in ASD produced a poorer representation. To confirm that group differences in silhouette value could not be explained by covariates of no interest (i.e. differences in scanning centre, age, group×age, IQ, and FD), we performed a regression analysis on silhouette values using the same covariates of no interest used for the univariate and multivariate analyses. Even after accounting for these covariates of no interest, there was still a significant group difference in silhouette value for the five cluster solution ($\beta=-0.0315$, $t(246)=-3.816$, $p=0.00017$, $pFDR=0.0033$; all other silhouette solutions $pFDR > 0.06$).

We created probability maps by enforcing the five cluster solution on each individual subject, and used hierarchical clustering to match single-subject clustering solutions of the left striatum to the group-specific template (see Section 2.3), thus establishing how often the group-specific clusters were identified in each individual subject. If a cluster at the individual level matched a cluster at the group level it was marked as 1, otherwise it was marked as 0. We then created probability maps for each cluster by summing binarised clusters from each individual subject. In order to remove overlapping voxels, probability maps were thresholded at > 25%, and a winner-take-all approach was used to assign overlapping voxels to the cluster with the greater probability. For example, if there was an overlapping voxel between the anterior and posterior putamen, and it had a 53% probability of being anterior and 47% probability of assigned to the posterior putamen, then the voxel was assigned to the anterior putamen cluster. Voxels with the exact same winning probability were not assigned to any cluster, however, this was not the case for many voxels. Details of the cluster peaks, size, average Dice similarity and number of matches are included in Supplemental Table 2. Our winner-takes-all probability maps showed that the left striatum of the TD group separated into five clusters: Caudate tail (Fig. 1b: blue), Caudate Nucleus (Fig. 1b: cyan), NAcc (Fig. 1b: green), Anterior Putamen (Fig. 1b: yellow), and Posterior Putamen (Fig. 1b: red). When applying the same approach to the ASD individuals, we found that one of the five clusters did not replicate in ASD individuals. Therefore, even though we enforced a five cluster solution at the single subject level, it “disappeared” in the winner-takes-all approach indicating that the forced five clusters resulted in a connectivity-based parcellation that was highly variable across ASD individuals. ASD individuals showed similar representations of the Caudate Tail (Fig. 1c: blue), Caudate Nucleus (Fig. 1c: cyan), and NAcc (Fig. 1c: green), however ASD individuals did not show a separation between anterior and posterior putamen, instead showing a single putamen cluster (Fig. 1c: red). The lack of a consistent separation in the putamen of individuals with ASD is the most likely reason for the significant deviation in silhouette value between groups. There were no significant group differences in the parcellation of the right striatum (see Supplemental Fig. 1).

After creating group-specific parcellations of the left striatum (Fig. 1b,c), we used hierarchical clustering to match clusters in the ASD and TD left striatum solutions. As expected the anterior putamen TD cluster (Fig. 1b, yellow) did not match any cluster in the ASD template. However, all the other TD clusters had a corresponding match in the ASD template (Caudate tail Dice similarity 0.55 (Blue); Anterior caudate Dice similarity 0.77 (cyan); Nucleus Accumbens Dice similarity 0.8 (green); Posterior putamen Dice similarity 0.86 (red)). We then used a regression analysis to establish whether there were group differences in the Dice similarity values that could not be explained by other covariates of no interest (i.e. centre, age, group×age, IQ, head movement). Dice similarity values for the caudate tail and anterior caudate were significantly larger in TD compared to ASD whereas Dice similarity values in the putamen were significantly larger in ASD compared to TD (Tail: $\beta=0.0298$, $t(157)=2.19$, $p=0.03$, $pFDR=0.04$; Anterior Caudate: $\beta=0.0361$, $t(194)=3.503$, $p=0.00057$, $pFDR=0.0011$; NAcc: $\beta=-0.0011$, $t(173)=-0.0871$, $p=0.9307$, $pFDR=0.93$; Putamen: $\beta=-0.0365$, $t(241)=-4.034$, $p=0.00007$, $pFDR=0.003$). These results highlight greater heterogeneity in the caudate tail and anterior caudate in ASD compared to TD. Even though there was significantly less heterogeneity in the putamen in ASD compared to TD, this is likely due to the absence of the anterior putamen cluster in ASD. There were no significant Group×Age interactions in Dice similarity.

Seed-to-voxel analyses

Cortico-Striatal connectivity fingerprints

Fig. 2 shows the average connectivity fingerprints for both groups for each of the striatal clusters and Supplemental Table 3 describes the peaks and anatomy of each connectivity fingerprint. The caudate tail

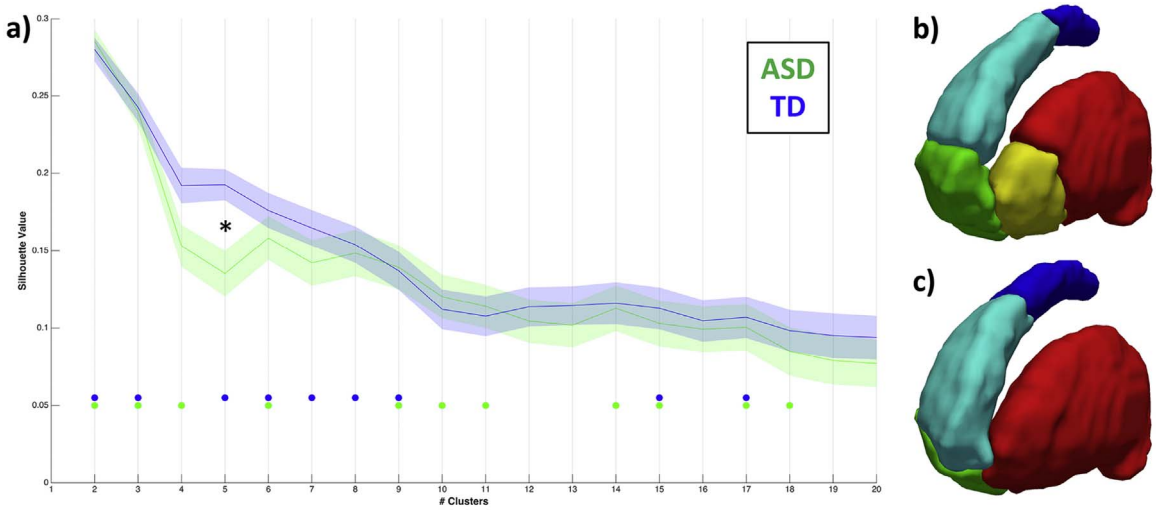

Fig. 1. Connectivity–based parcellation of the left striatum. A) Silhouette values for 2–20 clustering solutions in the left striatum for ASD and TD individuals. Blue (TD) and green (ASD) dots indicate a significant improvement in the clustering solution (i.e. a significant increase in the silhouette value) compared to the previous solution (i.e. the 2 cluster solution compared to the 3 cluster solution, the 3 cluster solution compared to the 4 cluster solution etc.). The black asterisk indicates a significant group difference in silhouette value. Significant improvements and differences in silhouette value were established using permutation testing (10,000 permutations) and corrected for multiple comparisons (FWE $p < 0.05$). B) and C) show the five cluster solutions of the left striatum in TD and ASD respectively. Five cluster solution probability maps were calculated for each group separately, and then a winner-takes-all approach was used to assign voxels to the cluster with the highest probability. It is important to highlight that C) only shows four clusters because one of the five clusters did not survive the winner-takes-all approach.

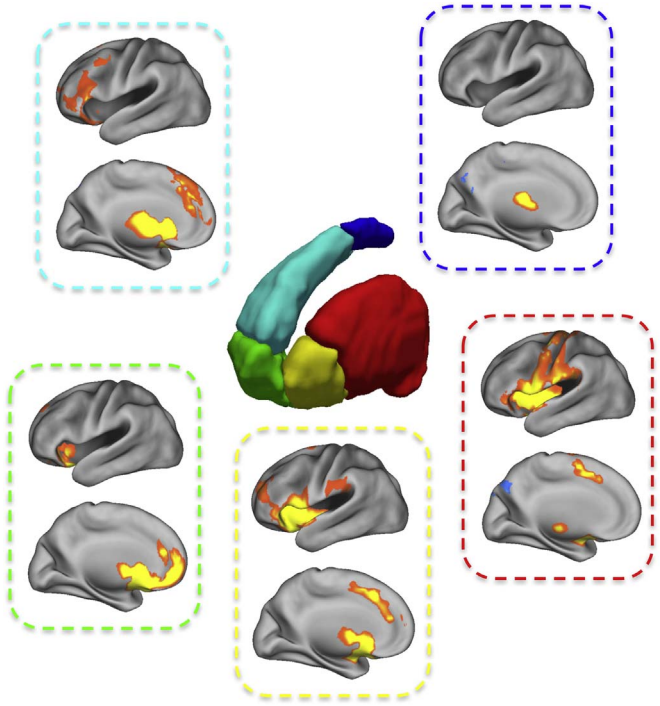

Fig. 2. Connectivity fingerprints of striatal clusters. Seed-to-voxel connectivity maps for each striatal cluster thresholded at $p < 0.05$ (cluster corrected, $Z > 3.1$, FWE $p < 0.05$). The colour code for boxes surrounding connectivity fingerprints corresponds to the colours for each striatal cluster.

only showed significant positive correlations with itself, and significant anticorrelations with precuneus. The anterior caudate cluster showed significant positive correlations with the inferior and middle frontal gyri as well as the anterior cingulate cortex (putatively Area 32d). The NAcc showed significant positive correlations with regions of the anterior cingulate cortex (putatively area 32pl), ventromedial prefrontal cortex, orbitofrontal cortex, and anterior insula. The anterior putamen cluster showed significant positive correlations with the inferior and middle frontal gyri, and the anterior cingulate cortex (putatively Area 32pl and the anterior rostral cingulate zone), however these connections do not overlap with the anterior caudate connectivity fingerprint. Additional unique connections were seen between the anterior putamen and the anterior insula, and inferior parietal lobule (putatively Area PF). The posterior putamen cluster showed strong connections with regions of the brain implicated in motor processing such as the precentral and postcentral gyri (areas 3, 4, and 6), the supplementary motor area (SMA), and the posterior insula (granular and dysgranular insula). The posterior putamen was also significantly anti-correlated with the cuneus and posterior cingulate cortex.

Group differences in cortico-striatal connectivity

There were no significant group differences in connectivity, however, there were some Group×Age interactions. Both the NAcc and the anterior putamen showed a Group×Age interaction with Frontal Pole (putatively FPl: Neubert et al., 2015, 2014). Connectivity between the FPl and the two striatal clusters decreased with age in the TD group, however this connectivity was static around zero in the ASD individuals (Fig. 3a,b). TD individuals also showed a significant increase in connectivity with age between the NAcc and the amygdala (Fig. 3c). Whilst these group differences in developmental trajectories are interesting, they do not explain why the putamen is segmented into anterior and posterior portions in TD but not in ASD.

A multivariate investigation of connectivity fingerprints

Given that hierarchical clustering is a multivariate technique (i.e. all voxels are considered simultaneously), it is possible that the traditional mass univariate approach is not capable of explaining the group differences we observed in connectivity-based parcellation. Here, we took a well-established multivariate approach (Mars et al., 2016) to try and explain why connectivity based parcellation of the striatum differs in ASD and TD individuals. These analyses were focussed on the anterior and posterior putamen.

Within group differences between anterior and posterior putamen connectivity fingerprints

We began by defining connectivity fingerprints as the peaks in a seed-to-voxel analysis (see Supplemental Fig. 2 and Supplemental Table 1). This gave us fifteen targets; 8 targets from the anterior putamen fingerprint and 7 targets from the posterior putamen

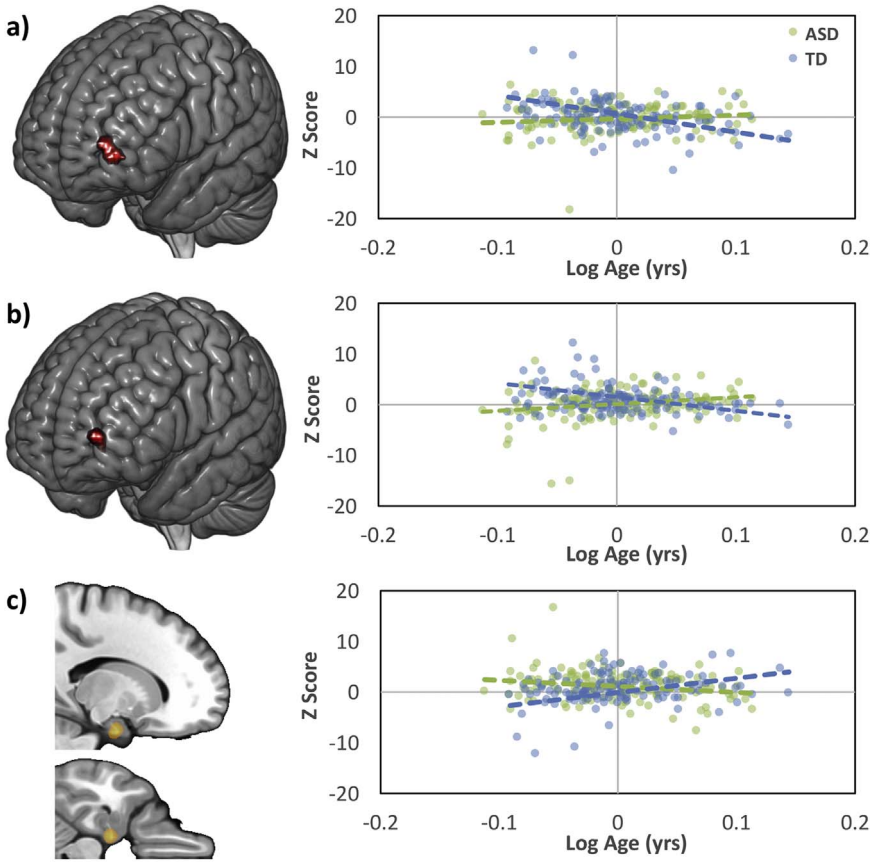

Fig. 3. Group differences in age-related changes in cortico-striatal connectivity. Group×Age interaction showing decreasing connectivity with age in TD individuals between the frontal pole (FPl) and the NAcc (A) and the FPl and the anterior putamen (B). C) Group×Age interaction showing increased connectivity with age between the NAcc and amygdala.

fingerprint. In every subject, we extracted the z transformed correlation value for each of fifteen targets. Specifically, the connectivity strength between the anterior putamen and all fifteen targets, and connectivity strength between the posterior putamen and all fifteen targets. We then calculated the Manhattan distance between connectivity fingerprints in each group separately. Using permutation testing (10,000 permutations), we showed that in both ASD and TD groups there was a significant difference between the fingerprints for the anterior and posterior putamen (ASD: Distance=2.367, $p < 0.001$; TD: Distance=2.5121, $p < 0.001$; see Fig. 4a).

Group differences in cortico-striatal connectivity fingerprints

Using the same multivariate approach, we calculated whether the anterior and posterior putamen connectivity fingerprints were different in ASD and TD individuals. There was a trend towards a group difference in the anterior putamen connectivity fingerprint (Distance=0.7942, p=0.09) and no group difference in the posterior putamen connectivity fingerprint (Distance=0.3472, p=0.7272). Lastly, we performed a Group×Seed interaction to see whether the difference between anterior and posterior putamen connectivity fingerprints was different between groups. This analysis revealed a significant group effect in the difference between anterior and posterior putamen connectivity fingerprints (Distance=0.8368, p=0.045; see Fig. 4b), and it is possible that differential connectivity between one or more of these targets is driving the group differences in connectivity-based parcellation.

To establish which connections were driving this Group×Seed interaction we performed logistic regression (Fig. 4c). The posterior cingulate cortex (PCC: β=0.2174, t(244)=2.1376, p=0.0326, pFDR=0.13), granular portion of the Insula (Insula IG1: β=0.1693, t(244)=2.4474, p=0.0144, pFDR= 0.0767), SMA (β=−0.168, t(244) =−2.503, p=0.0123, pFDR=0.0767), and precuneus (β=−0.359, t(244) =−3.3957, p=0.00068, pFDR=0.011) were all identified as significant group predictors. The difference between anterior and posterior putamen resting connectivity with the PCC, posterior insula, and precuneus was greater in TD compared to ASD, whereas the difference between anterior and posterior putamen resting connectivity with the SMA was greater in ASD compared to TD (see Supplemental Fig. 3). Thus, the separation between anterior and posterior putamen in TD could be driven by these connectivity fingerprint differences.

Discussion

Cortico-striatal circuitry has been linked to cognitive, social, and motor functions, all of which are known to be effected in ASD. Although a number of studies have shown increased striatal volume in ASD, as well as increased cortico-striatal connectivity in ASD, this is the first study that has identified differences in the organisation of cortico-striatal circuitry in ASD. Using connectivity-based parcellation, we showed that the putamen separated into anterior and posterior segments in TD individuals, however, the putamen remained as one cluster in ASD. A traditional mass univariate analysis highlighted several developmental changes in cortico-striatal connectivity in TD, whereas individuals with ASD did not show any age-related changes in cortico-striatal connectivity. However, these results could not explain why the putamen was segmented in TD but not in ASD. Lastly, we used a multivariate approach to compare anterior and posterior putamen connectivity fingerprints in ASD and TD. These analyses suggest that the segregation of the anterior and posterior putamen in TD, but not in ASD, was driven by differential connectivity with the PCC, precuneus, posterior insula, and SMA.

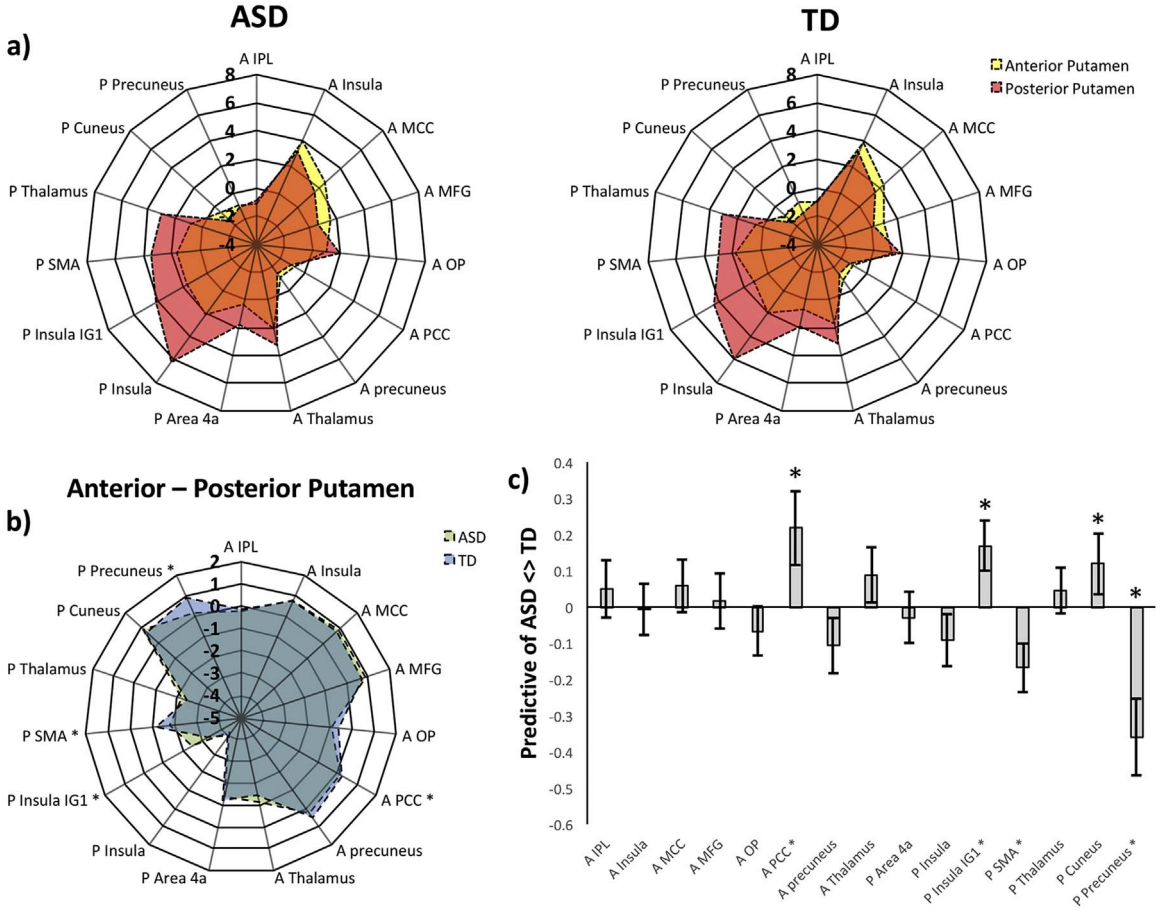

Fig. 4. Multivariate approach to matching connectivity fingerprints. A) Connectivity fingerprints showing the connectivity strength between seeds (anterior and posterior putamen) and targets (labels beginning with A are taken from the anterior putamen seed-to-voxel analysis whilst labels beginning with P were taken from the posterior putamen seed-to-voxel analysis). A measurement of distance (Manhattan) showed that in both TD and ASD individuals the anterior and posterior putamen have unique connectivity fingerprints. B) Connectivity fingerprint of the difference in connectivity between the anterior and posterior putamen in ASD and TD. This illustrates the Group×Seed interaction in connectivity fingerprints. C) Beta weights of a logistic regression testing which connections were driving the Group×Seed interaction (* next to the label and above the bar indicates significant predictive ability, $p < 0.05$ uncorrected).

Group differences in the architecture of the cortico-striatal system

Although previous studies have highlighted differences in striatal volume and connectivity, this is the first study to suggest that the architecture of the cortico-striatal system is different in ASD compared to TD. Connectivity-based parcellation revealed that the putamen separated into anterior and posterior segments in TD, however, in ASD the putamen remained one single cluster. Previous connectivity-based parcellation studies have segmented the putamen in 1–6 regions using task-independent measures such as RS-fMRI and diffusion imaging (Choi et al., 2012; Janssen et al., 2015; Jaspers et al., 2016; Jung et al., 2014; Tziortzi et al., 2014). In this study, similar to Jaspers et al. (2016), we found that the two or three cluster parcellation of the striatum (splitting the caudate nucleus, NAcc, and putamen) was the most representative solution in both groups and hemispheres. However, group differences in the parcellation of the left striatum were apparent for the five cluster solution (Fig. 1). One caveat raised by Jaspers et al. (2016), was that while simpler clustering solutions will have higher inter-subject replication, individual variability might only be seen when the parcellation scheme is more complex. Here, we show that the fundamental anatomical parcellation of the striatum (i.e. splitting the caudate, NAcc, and putamen) was the same for ASD and TD individuals, however, differences between groups became apparent at the five cluster solution. Interestingly, the only study to partition the striatum using task-based information also showed a five cluster segmentation of the striatum (Pauli et al., 2016). Comparing our results to those of Pauli et al. (2016) shows that their five cluster parcellation of the striatum bares a remarkable resemblance to our five cluster parcellation in TD individuals, however, it was clear that in ASD the anterior putamen cluster was absent. Pauli et al. (2016) suggested that the anterior putamen cluster corresponded to social and language functions, specifically the anterior putamen was associated with psychological terms “read”, “vocal”, and “empathic”. We therefore suggest that the absence of functional specialization in the left anterior putamen in ASD could contribute to language deficits seen in the disorder.

The Left Hemisphere Dysfunction (LHD) theory of Autism was previously proposed because individuals with ASD show deficits in tasks typically ascribed to the left hemisphere such as language, whilst performance on tasks typically ascribed to the right hemisphere such as visual-spatial abilities are relatively spared (McCann, 1981). Whilst several studies have shown that a lack of functional lateralization in ASD corresponds to deficits in language (Floris et al., 2016b; Mellet et al., 2014), several other studies have suggested that these lateralization effects go beyond the domain of language and additionally impact on other brain networks. For example, Cardinale et al. (2013) used RS-fMRI to assess functional asymmetry and showed rightward bias in BOLD activity for a range of resting state networks including visual, motor, and executive (fronto-parietal) networks. Floris et al. (2016a) also highlighted asymmetries in resting connectivity, specifically a rightward bias in resting motor connectivity but not in visual brain regions or the default mode network (DMN). The degree of rightward

bias in motor circuits in ASD was also a marker of poorer motor performance as measured by neuropsychological tools. Rinehart et al. (2002) posited that deficits in executive functions seen in ASD could be attributed to maladaptive processing of the left fronto-striatal system because individuals with ASD showed a greater deficit in executive functions performed in the right hemispace (i.e. left fronto-striatal circuitry). These same ASD individuals did not show any lateralization effects in a visual control task. Several studies have proposed that brain lateralization (both structural and functional) is advantageous from an evolutionary standpoint as it reduces redundant cognitive processing (Floris et al., 2016b; Hugdahl, 2011). This link between lateralization and performance has been shown in both the motor domain (Barber et al., 2012; Floris et al., 2016a), and the cognitive domain (Gotts et al., 2013; Mellet et al., 2014). Our results, in line with several other studies, highlight a lack of asymmetry in ASD, and provide further evidence for cortico-striatal contributions to language.

There is increasing evidence to suggest that cortico-striatal circuits contribute to speech production by aiding word selection and inhibiting irrelevant competing information for language, similar to the way the basal ganglia has been shown to facilitate action selection (Friend and Kravitz, 2014; Price, 2010). It is therefore possible that variations in cortico-striatal circuits could lead to deficits in restricted and repetitive behaviour such as stereotyped language. Volumetric studies by Langen et al. (2013, 2009) and Hollander et al. (2005) have associated increased striatal volume with the severity of restrictive and repetitive behaviours in ASD. In a series of studies Radulescu et al. (2013a, 2013b) previously found that in Aspergers syndrome (AS), but not in controls, the volume of the ventral striatum and anterior putamen corresponded to abnormalities in cortical gray matter homogeneity. In a follow-up study, Radulescu et al. (2013b) had the same AS individuals perform a language generation task (verbal fluency) and used dynamic causal modelling to highlight differences in cortico-striatal connectivity. Whilst individuals with AS revealed a reliance on bottom-up (stimulus-driven) connections from the precuneus to the caudate and onto the bilateral inferior frontal gyri, the flow of information went in the opposite direction in TD participants (i.e. bilateral inferior frontal gyri to the caudate to the precuneus) highlighting a greater degree of top-down cognitive control. These results are in line with recent Bayesian accounts of ASD that have suggested individuals with ASD place too great an emphasis on stimulus information, without placing much emphasis on prior knowledge (Lawson et al., 2014; Pellicano and Burr, 2012; Van de Cruys et al., 2014). Within this Bayesian framework, Friston et al. (2016, 2014) hypothesised a general role of the striatum in terms of optimal policy/action selection. Whilst our findings highlight cortico-striatal deficits in resting-state functional connectivity, future studies will be required to assess whether language deficits commonly seen in ASD could be explained by problems with policy/action selection.

Multivariate approaches to connectivity fingerprint matching

Our multivariate approach to matching connectivity fingerprints, combined with logistic regression analysis, confirmed that group differences between the anterior and posterior putamen were largely driven by connectivity with the precuneus, PCC, left granular insula (IG1), and SMA. It is important to reiterate that these effects were not seen using traditional mass univariate approaches, however, given that hierarchical clustering is a multivariate technique (i.e. all voxels are considered simultaneously) it is logical that another multivariate approach was necessary to establish which connections were driving the group differences in connectivity-based parcellation. It has been suggested that multivariate approaches may be more sensitive to classification and diagnosis of psychiatric conditions than mass univariate approaches (Buckholtz and Meyer-Lindenberg, 2012; Jafri et al., 2008; Kassraian Fard et al., 2016; Uddin et al., 2011). For example, Uddin et al. (2011) examined group differences in gray matter concentration using voxel based morphometry (VBM) and similarly found that multivariate approaches were more sensitive to detecting group differences than traditional mass-univariate approaches. We do not wish to suggest here that one approach is better than another, since it is clear that multivariate and univariate approaches can be complementary (Mars et al., 2016).

In this case a multivariate approach, matching connectivity fingerprints, highlighted that connectivity differences between the precuneus, PCC, left posterior (granular) insula (IG1), and SMA had differential anterior and posterior putamen connectivity fingerprints in TD. However, it is important to reiterate that only group differences in the precuneus survived correction for multiple comparisons. The precuneus and PCC are considered to be part of the default mode network (DMN), a system of brain regions associated with social cognition and theory of mind processes (Buckner et al., 2008). A number of studies have focussed on the DMN in ASD and shown reduced resting state activity in the precuneus/PCC (Assaf et al., 2010; Di Martino et al., 2014b; Lynch et al., 2013), however, some other studies have not been able to replicate these findings (Balsters et al., 2016; Tyszka et al., 2014). As in our study, Lynch et al. (2013) found increased connectivity between the precuneus and the caudate nucleus (potentially overlapping with the anterior putamen) in TD individuals. Although the striatum is not considered to be part of the DMN, Uddin et al. (2009) previously showed that striatal activity, along with the anterior cingulate cortex and insula, was negatively correlated with the posterior portion of the default mode network (precuneus/posterior cingulate cortex). Using the same ABIDE dataset used in this study, Di Martino et al. (2014b) used a number of resting state metrics (ReHo: regional homogeneity, VMHC: voxel-matched homotopic connectivity, DC: degree centrality, and fALFF: fractional amplitude of low-frequency fluctuations) to investigate resting state connectivity in ASD. These analyses identified significant group differences in three out of four of these metrics (ReHo, VMHC, and DC) in the left posterior insula and two out of four group differences (ReHo, VMHC) in the precuneus/PCC as well as two additional seed-to-voxel analyses of the PCC and medial prefrontal cortex. Although Di Martino et al. (2014b) did not report any group differences in the SMA, Cerliani et al. (2015) also used the ABIDE dataset and found increased connectivity in ASD between the basal ganglia and a dorsomedial motor network (dorsal primary sensory cortex, dorsal primary motor cortex, and medial premotor cortex). In addition, Cerliani et al. (2015) found that increased connectivity in this network in ASD indexed social symptom severity as measured by the social responsiveness scale (Constantino et al., 2003).

The insula is traditionally separated into three regions based on its cytoarchitectonic properties; agranular cortex (anterior insula), a middle dysgranular cortex (middle insula) and a posterior granular cortex (posterior insula) (Mesulam and Mufson, 1982). In line with the findings of this study, animal tracer studies and human neuroimaging studies have shown that the posterior insula has connections to the SMA and putamen and as such the posterior insula is often associated with action execution and sensory perception (Kelly et al., 2012; Mesulam and Mufson, 1982). In contrast, the anterior insula cortex has often been linked to empathy and social processing (Di Martino et al., 2009a; Lockwood, 2016; Uddin and Menon, 2009). Lockwood (2016) proposed that a network of brain regions including the anterior insula and gyrus of the anterior cingulate cortex (ACCg) are essential for processing information about others. These ideas were recently supported by Balsters et al. (2017) who showed that the ACCg signalled unexpected outcomes exclusively for another person (not for their own unexpected outcomes or unexpected outcomes for a computer) in TD but not in an age- and IQ-matched group of individuals with ASD. Interestingly, Di Martino et al. (2009b) showed that anti-correlations in resting connectivity between the ACCg and the middle/posterior insula were a marker of social deficits in TD individuals. Although the anterior insula is often considered to be important for empathy and

understanding others, whilst the posterior insula is important for personal bodily sensation, it is possible that interactions between 'social' cingulo-insula loops (i.e. anterior insula and ACCg) and 'motor' cingulo-insula loops (i.e. SMA and posterior insula) impact on social processing. The connectivity-based parcellation methods employed in this study could help to identify potential heterogeneity in the functions of the insula in ASD.

Developmental trajectories in cortico-striatal connectivity

It is becoming increasingly important to consider ASD research within a developmental framework (Picci and Scherf, 2015; Uddin et al., 2013). Uddin et al. (2013) proposed that individuals with ASD may show hyper-active RS-fMRI connectivity in childhood, which combined with a more rigid developmental profile could lead to no observable group differences between ASD and TD individuals during adolescence, and hypo-active RS-fMRI connectivity during adulthood. The Group×Age interactions in cortico-striatal connectivity appear to support this model of developmental rigidity. Functional connectivity between the NAcc and the lateral frontal pole (FPl), and the anterior putamen and same FPl region, decreased with age in TD but stayed constant in ASD. Functional connectivity between the NAcc and amygdala increased with age in TD but stayed constant in ASD. Although it is interesting that cortico-striatal connectivity stays constant in ASD, it would be premature to suggest that developmental rigidity is a general feature of ASD. In the present study, we did not include non-linear age regressors that could describe more dramatic developmental changes during adolescence. Both Uddin et al. (2013) and Picci and Scherf (2015) have proposed that adolescence could provide a "second hit" on an already weak system that leads to a marked decline in adaptive functioning during adolescence. In addition, a number of RS-fMRI studies have shown age-related increases in connectivity in ASD (Balsters et al., 2016; Cerliani et al., 2015). For example, using the same dataset, Balsters et al. (2016) found increased age-related connectivity in ASD between the anterior middle cingulate cortex and the right middle frontal gyrus whilst these areas showed decreased connectivity with age in TD. Similarly, Cerliani et al. (2015) showed age-related increases in functional connectivity between the anterior cerebellum (putatively motor lobules; Balsters et al., 2014) and the superior temporal sulcus and inferior frontal gyrus in ASD. However, consistent with the findings of this study Cerliani et al. (2015) also showed that cortico-striatal connectivity did not change with age in ASD. Therefore, it is possible that developmental rigidity is only a feature of the cortico-striatal system and that other brain circuits may develop differently. In order to generate a more robust developmental framework in ASD we require longitudinal datasets that will demonstrate age-related changes in connectivity within individuals. Developmental trajectories can often be obscured in cross-sectional analyses, as demonstrated by Nyberg et al. (2010) who showed increased prefrontal cortex activity from 45 to 80 yrs of age, however, a longitudinal analysis of the same subjects clearly showed a decline in prefrontal cortex activity with age. The inclusion of longitudinal datasets, as well as data for ASD individuals below 7 years old, would greatly improve our understanding of developmental changes in ASD (Di Martino et al., 2014a; Uddin et al., 2013).

All three of these regions showing Group×Age interactions (NAcc, FPl, and amygdala) were highlighted as key regions in the Social Motivation Theory of ASD (Chevallier et al., 2012). The Social Motivation Theory of ASD suggests that ASD pathology may result from maladaptive interactions between social brain regions and regions involved in reward and motivation. A number of studies investigating the social and monetary rewards in ASD have shown differences in amygdala, NAcc, and frontal pole activity. Richey et al. (2014) compared the anticipation and receipt of social outcomes (smiling faces) with monetary outcomes in controls, ASD, and social anxiety disorder (SAD). They found reduced activity in the NAcc during the anticipation of social and monetary rewards in ASD, however, the SAD group only showed reduced NAcc activity during the anticipation of social outcomes. Left amygdala responses to both the anticipation and receipt of social outcomes also differentiated SAD and ASD groups. Kohls et al. (2013) also showed reduced activation in the NAcc when money, but not when social rewards were at stake, and reduced amygdala activity in response to both monetary and social rewards in ASD. Scott-Van Zeeland et al. (2010a) found greater FPl activity for positive compared to negative monetary rewards in ASD, but greater NAcc and FPl activity in TD compared to ASD during social learning. Both the FPl and the amygdala have also been linked to social and emotional decision making (Volman et al., 2011a, 2011b). In two studies by Volman et al. (2011b, 2011a) participants had to perform a social approach-avoidance task performing both congruent movements (i.e. towards a happy face and away from an angry face), or incongruent movements (i.e. towards an angry face and away from a happy face). In Volman et al. (2011b), participants with less endogenous testosterone showed increased activity in the left FPl for incongruent compared to congruent trials whilst individuals with more endogenous testosterone did not show any difference in FPl response between these conditions. Levels of endogenous testosterone also modulated connectivity between the left FPl and bilateral amygdala. In a separate study, Volman et al. (2011a) used continuous theta-burst stimulation (cTBS) of the left FPl before performing the same task. The application of cTBS increased the error rate on incongruent trials, reduced FPl activity, and increased amygdala activity. All these studies highlight how the NAcc, FPl, and amygdala are crucial to social motivation and decision making. To our knowledge, none of the aforementioned studies have investigated developmental trajectories during ASD, however, we propose that these age-related changes in connectivity during typical development likely reflect aspects of social development. A greater understanding of these developmental changes in connectivity will be crucial for developing novel therapeutic interventions.

Conclusions

Here, we used connectivity-based parcellation to investigate the architecture and organisation of the cortico-striatal system in ASD. Our novel approach revealed differences in the parcellation of the striatum in ASD. Specifically, the putamen was found to be one single structure in ASD, whereas this was split into anterior and posterior segments in a matched TD group. An analysis of the connectivity fingerprints revealed that the group differences in clustering were driven by differential connectivity between anterior and posterior segments of the putamen and the SMA, precuneus, PCC, and posterior insula. Our novel approach for analysing resting state fMRI in clinical populations has provided clear evidence that cortico-striatal circuits are organized differently in ASD as compared to healthy participants. Based on previous task-based segmentations of the striatum, we believe that the anterior putamen cluster present in TD, but not in ASD, likely contributes to social and language processes. Whilst it is currently not possible to reliably investigate variability in clinical features using the ABIDE database, we hope that the inclusion of the second wave of ABIDE (ABIDE II: http://fcon_1000.projects.nitrc.org/indi/abide/abide_II.html) might provide the consistency and sample size necessary to begin linking RS-fMRI connectivity to ASD symptom severity, including whether cortico-striatal organisation predicts social and language deficits in ASD.

Acknowledgements

N.W. is supported by an ETH Research Grant (ETH-38 16-2). D.M. is supported by a Sir Henry Dale award of the Wellcome Trust and the Royal Society (grant number 101253/Z/13/Z).

Appendix A. Supplementary material

Supplementary data associated with this article can be found in the online version at http://dx.doi.org/10.1016/j.neuroimage.2017.02.019.

References

Alexander, G.E., DeLong, M.R., Strick, P.L., 1986. Parallel organization of functionally segregated circuits linking basal ganglia and cortex. Annu. Rev. Neurosci. 9, 357–381. http://dx.doi.org/10.1146/annurev.ne.09.030186.002041.

Amunts, K., Zilles, K., 2015. Architectonic Mapping of the Human Brain beyond Brodmann. Neuron 88, 1086–1107. http://dx.doi.org/10.1016/j.neuron.2015.12.001.

Ashburner, J., 2007. A fast diffeomorphic image registration algorithm. NeuroImage 38, 95–113. http://dx.doi.org/10.1016/j.neuroimage.2007.07.007.

Assaf, M., Jagannathan, K., Calhoun, V.D., Miller, L., Stevens, M.C., Sahl, R., O'Boyle, J.G., Schultz, R.T., Pearlson, G.D., 2010. Abnormal functional connectivity of default mode sub-networks in autism spectrum disorder patients. NeuroImage 53, 247–256. http://dx.doi.org/10.1016/j.neuroimage.2010.05.067.

Balsters, J., Apps, M.A.J., Bolis, D., Lehner, R., Gallagher, L., Wenderoth, N., 2017. Disrupted prediction errors index social deficits in autism spectrum disorder. Brain 140, 235–246. http://dx.doi.org/10.1093/brain/aww287.

Balsters, J., Laird, A.R., Fox, P.T., Eickhoff, S.B., 2014. Bridging the gap between functional and anatomical features of cortico-cerebellar circuits using meta-analytic connectivity modeling. Hum. Brain Mapp. 35, 3152–3169. http://dx.doi.org/10.1002/hbm.22392.

Balsters, J., Mantini, D., Apps, M.A.J., Eickhoff, S.B., Wenderoth, N., 2016. Connectivity-based parcellation increases network detection sensitivity in resting state fMRI: an investigation into the cingulate cortex in autism. NeuroImage: Clin. 11, 494–507. http://dx.doi.org/10.1016/j.nicl.2016.03.016.

Balsters, J., Robertson, I.H., Calhoun, V.D., 2013. BOLD frequency power indexes working memory performance. Front. Hum. Neurosci. 7, 207. http://dx.doi.org/10.3389/fnhum.2013.00207.

Barber, A.D., Srinivasan, P., Joel, S.E., Caffo, B.S., Pekar, J.J., Mostofsky, S.H., 2012. Motor "Dexterity?": evidence that left hemisphere lateralization of motor circuit connectivity is associated with better motor performance in children. Cereb. Cortex 22, 51–59. http://dx.doi.org/10.1093/cercor/bhr062.

Baria, A.T., Baliki, M.N., Parrish, T., Apkarian, A.V., 2011. Anatomical and functional assemblies of brain BOLD oscillations. J. Neurosci. 31, 7910–7919. http://dx.doi.org/10.1523/JNEUROSCI.1296-11.2011.

Buckholtz, J.W., Meyer-Lindenberg, A., 2012. Psychopathology and the human connectome: toward a transdiagnostic model of risk for mental illness. Neuron 74, 990–1004. http://dx.doi.org/10.1016/j.neuron.2012.06.002.

Buckner, R.L., Andrews-Hanna, J.R., Schacter, D.L., 2008. The brain's default network: anatomy, function, and relevance to disease. Ann. N.Y. Acad. Sci. 1124, 1–38. http://dx.doi.org/10.1196/annals.1440.011.

Cardinale, R.C., Shih, P., Fishman, I., Ford, L.M., Müller, R.-A., 2013. Pervasive rightward asymmetry shifts of functional networks in autism spectrum disorder. JAMA Psychiatry 70, 975–982. http://dx.doi.org/10.1001/jamapsychiatry.2013.382.

Cerliani, L., Mennes, M., Thomas, R.M., Di Martino, A., Thioux, M., Keysers, C., 2015. Increased functional connectivity between subcortical and cortical resting-state networks in autism spectrum disorder. JAMA Psychiatry 72, 767–777. http://dx.doi.org/10.1001/jamapsychiatry.2015.0101.

Chai, X.J., Castañón, A.N., Ongür, D., Whitfield-Gabrieli, S., 2012. Anticorrelations in resting state networks without global signal regression. NeuroImage 59, 1420–1428. http://dx.doi.org/10.1016/j.neuroimage.2011.08.048.

Chevallier, C., Kohls, G., Troiani, V., Brodkin, E.S., Schultz, R.T., 2012. The social motivation theory of autism. Trends Cogn. Sci. 16, 231–239. http://dx.doi.org/10.1016/j.tics.2012.02.007.

Choi, E.Y., Yeo, B.T.T., Buckner, R.L., 2012. The organization of the human striatum estimated by intrinsic functional connectivity. J. Neurophysiol. 108, 2242–2263. http://dx.doi.org/10.1152/jn.00270.2012.

Constantino, J.N., Davis, S.A., Todd, R.D., Schindler, M.K., Gross, M.M., Brophy, S.L., Metzger, L.M., Shoushtari, C.S., Splinter, R., Reich, W., 2003. Validation of a brief quantitative measure of autistic traits: comparison of the social responsiveness scale with the autism diagnostic interview-revised. J. Autism Dev. Disord. 33, 427–433.

Deen, B., Pelphrey, K., 2012. Perspective: brain scans need a rethink. Nature 491. http://dx.doi.org/10.1038/491S20a.

Delmonte, S., Balsters, J., McGrath, J., Fitzgerald, J., Brennan, S., Fagan, A.J., Gallagher, L., 2012. Social and monetary reward processing in autism spectrum disorders. Mol. Autism 3, 7. http://dx.doi.org/10.1186/2040-2392-3-7.

Delmonte, S., Gallagher, L., O'Hanlon, E., McGrath, J., Balsters, J., 2013. Functional and structural connectivity of frontostriatal circuitry in autism spectrum disorder. Front. Hum. Neurosci. 7, 430. http://dx.doi.org/10.3389/fnhum.2013.00430.

Di Martino, A., Fair, D.A., Kelly, C., Satterthwaite, T.D., Castellanos, F.X., Thomason, M.E., Craddock, R.C., Luna, B., Leventhal, B.L., Zuo, X.-N., Milham, M.P., 2014a. Unraveling the miswired connectome: a developmental perspective. Neuron 83, 1335–1353. http://dx.doi.org/10.1016/j.neuron.2014.08.050.

Di Martino, A., Kelly, C., Grzadzinski, R., Zuo, X.-N., Mennes, M., Mairena, M.A., Lord, C., Castellanos, F.X., Milham, M.P., 2011. Aberrant striatal functional connectivity in children with autism. Biol. Psychiatry 69, 847–856. http://dx.doi.org/10.1016/j.biopsych.2010.10.029.

Di Martino, A., Ross, K., Uddin, L.Q., Sklar, A.B., Castellanos, F.X., Milham, M.P., 2009a. Functional brain correlates of social and nonsocial processes in autism spectrum disorders: an activation likelihood estimation meta-analysis. Biol. Psychiatry 65, 63–74. http://dx.doi.org/10.1016/j.biopsych.2008.09.022.

Di Martino, A., Shehzad, Z., Kelly, C., Roy, A.K., Gee, D.G., Uddin, L.Q., Gotimer, K., Klein, D.F., Castellanos, F.X., Milham, M.P., 2009b. Relationship between cingulo-insular functional connectivity and autistic traits in neurotypical adults. Am. J. Psychiatry 166, 891–899. http://dx.doi.org/10.1176/appi.ajp.2009.08121894.

Di Martino, A., Yan, C.-G., Li, Q., Denio, E., Castellanos, F.X., Alaerts, K., Anderson, J.S., Assaf, M., Bookheimer, S.Y., Dapretto, M., Deen, B., Delmonte, S., Dinstein, I., Ertl-Wagner, B., Fair, D.A., Gallagher, L., Kennedy, D.P., Keown, C.L., Keysers, C., Lainhart, J.E., Lord, C., Luna, B., Menon, V., Minshew, N.J., Monk, C.S., Mueller, S., Müller, R.-A., Nebel, M.B., Nigg, J.T., O'Hearn, K., Pelphrey, K.A., Peltier, S.J., Rudie, J.D., Sunaert, S., Thioux, M., Tyszka, J.M., Uddin, L.Q., Verhoeven, J.S., Wenderoth, N., Wiggins, J.L., Mostofsky, S.H., Milham, M.P., 2014b. The autism brain imaging data exchange: towards a large-scale evaluation of the intrinsic brain architecture in autism. Mol. Psychiatry 19, 659–667. http://dx.doi.org/10.1038/mp.2013.78.

Dice, L.R., 1945. Measures of the amount of ecologic association between species. Ecology 26, 297. http://dx.doi.org/10.2307/1932409.

Dichter, G., Adolphs, R., 2012. Reward processing in autism: a thematic series. J Neurodev. Disord. 4, 20. http://dx.doi.org/10.1186/1866-1955-4-20.

Draganski, B., Kherif, F., Klöppel, S., Cook, P.A., Alexander, D.C., Parker, G.J.M., Deichmann, R., Ashburner, J., Frackowiak, R.S.J., 2008. Evidence for segregated and integrative connectivity patterns in the human Basal Ganglia. J. Neurosci. 28, 7143–7152. http://dx.doi.org/10.1523/JNEUROSCI.1486-08.2008.

Eickhoff, S.B., Heim, S., Zilles, K., Amunts, K., 2006. Testing anatomically specified hypotheses in functional imaging using cytoarchitectonic maps. NeuroImage 32, 570–582. http://dx.doi.org/10.1016/j.neuroimage.2006.04.204.

Eickhoff, S.B., Paus, T., Caspers, S., Grosbras, M.-H., Evans, A.C., Zilles, K., Amunts, K., 2007. Assignment of functional activations to probabilistic cytoarchitectonic areas revisited. NeuroImage 36, 511–521. http://dx.doi.org/10.1016/j.neuroimage.2007.03.060.

Eickhoff, S.B., Stephan, K.E., Mohlberg, H., Grefkes, C., Fink, G.R., Amunts, K., Zilles, K., 2005. A new SPM toolbox for combining probabilistic cytoarchitectonic maps and functional imaging data. NeuroImage 25, 1325–1335. http://dx.doi.org/10.1016/j.neuroimage.2004.12.034.

Eickhoff, S.B., Thirion, B., Varoquaux, G., Bzdok, D., 2015. Connectivity-based parcellation: critique and implications. Hum. Brain Mapp. 36, 4771–4792. http://dx.doi.org/10.1002/hbm.22933.

Floris, D.L., Barber, A.D., Nebel, M.B., Martinelli, M., Lai, M.-C., Crocetti, D., Baron-Cohen, S., Suckling, J., Pekar, J.J., Mostofsky, S.H., 2016a. Atypical lateralization of motor circuit functional connectivity in children with autism is associated with motor deficits. Mol. Autism 7, 35. http://dx.doi.org/10.1186/s13229-016-0096-6.

Floris, D.L., Lai, M.-C., Auer, T., Lombardo, M.V., Ecker, C., Chakrabarti, B., Wheelwright, S.J., Bullmore, E.T., Murphy, D.G.M., Baron-Cohen, S., Suckling, J., 2016b. Atypically rightward cerebral asymmetry in male adults with autism stratifies individuals with and without language delay. Hum. Brain Mapp. 37, 230–253. http://dx.doi.org/10.1002/hbm.23023.

Friend, D.M., Kravitz, A.V., 2014. Working together: basal ganglia pathways in action selection. Trends Neurosci. 37, 301–303. http://dx.doi.org/10.1016/j.tins.2014.04.004.

Friston, K., FitzGerald, T., Rigoli, F., Schwartenbeck, P., O'Doherty, J., Pezzulo, G., 2016. Active inference and learning. Neurosci. Biobehav. Rev. 68, 862–879. http://dx.doi.org/10.1016/j.neubiorev.2016.06.022.

Friston, K., Schwartenbeck, P., FitzGerald, T., Moutoussis, M., Behrens, T., Dolan, R.J., 2014. The anatomy of choice: dopamine and decision-making. Philos. Trans. R. Soc. B: Biol. Sci. 369. http://dx.doi.org/10.1098/rstb.2013.0481.

Friston, K.J., Williams, S., Howard, R., Frackowiak, R.S., Turner, R., 1996. Movement-related effects in fMRI time-series. Magn. Reson. Med. 35, 346–355.

Fuccillo, M.V., 2016. Striatal circuits as a common node for autism pathophysiology. Front. Neurosci. 10, 27. http://dx.doi.org/10.3389/fnins.2016.00027.

Gordon, E.M., Laumann, T.O., Adeyemo, B., Huckins, J.F., Kelley, W.M., Petersen, S.E., 2014. Generation and evaluation of a cortical area parcellation from resting-state correlations. Cereb. Cortex. http://dx.doi.org/10.1093/cercor/bhu239, (bhu239).

Gotts, S.J., Jo, H.J., Wallace, G.L., Saad, Z.S., Cox, R.W., Martin, A., 2013. Two distinct forms of functional lateralization in the human brain. Proc. Natl. Acad. Sci. 110, E3435–E3444. http://dx.doi.org/10.1073/pnas.1302581110.

Hahamy, A., Behrmann, M., Malach, R., 2015. The idiosyncratic brain: distortion of spontaneous connectivity patterns in autism spectrum disorder. Nat. Neurosci.. http://dx.doi.org/10.1038/nn.3919.

Haznedar, M.M., Buchsbaum, M.S., Hazlett, E.A., LiCalzi, E.M., Cartwright, C., Hollander, E., 2006. Volumetric analysis and three-dimensional glucose metabolic mapping of the striatum and thalamus in patients with autism spectrum disorders. Am. J Psychiatry 163, 1252–1263. http://dx.doi.org/10.1176/appi.ajp.163.7.1252.

Hollander, E., Anagnostou, E., Chaplin, W., Esposito, K., Haznedar, M.M., Licalzi, E., Wasserman, S., Soorya, L., Buchsbaum, M., 2005. Striatal volume on magnetic resonance imaging and repetitive behaviors in autism. BPS 58, 226–232. http://dx.doi.org/10.1016/j.biopsych.2005.03.040.

Hugdahl, K., 2011. Fifty years of dichotic listening research – still going and going and.... Brain Cogn. 76, 211–213. http://dx.doi.org/10.1016/j.bandc.2011.03.006.

Jafri, M.J., Pearlson, G.D., Stevens, M., Calhoun, V.D., 2008. A method for functional network connectivity among spatially independent resting-state components in schizophrenia. NeuroImage 39, 1666–1681. http://dx.doi.org/10.1016/j.neuroimage.2007.11.001.

Janssen, R.J., Jylänki, P., Kessels, R.P.C., van Gerven, M.A.J., 2015. Probabilistic model-

based functional parcellation reveals a robust, fine-grained subdivision of the striatum. NeuroImage 119, 398–405. http://dx.doi.org/10.1016/j.neuroimage.2015.06.084.
Jaspers, E., Balsters, J., Kassraian Fard, P., Mantini, D., Wenderoth, N., 2016. Corticostriatal connectivity fingerprints: probability maps based on resting-state functional connectivity. Hum. Brain Mapp.. http://dx.doi.org/10.1002/hbm.23466.
Jenkinson, M., Beckmann, C.F., Behrens, T.E.J., Woolrich, M.W., Smith, S.M., 2012. FSL. NeuroImage 62, 782–790. http://dx.doi.org/10.1016/j.neuroimage.2011.09.015.
Jung, W.H., Jang, J.H., Park, J.W., Kim, E., Goo, E.-H., Im, O.-S., Kwon, J.S., 2014. Unravelling the intrinsic functional organization of the human striatum: a parcellation and connectivity study based on resting-state FMRI. PLoS One 9, e106768. http://dx.doi.org/10.1371/journal.pone.0106768.
Kassraian Fard, P., Matthis, C., Balsters, J., Maathuis, M.H., Wenderoth, N., 2016. Promises, pitfalls, and basic guidelines for applying machine learning classifiers to psychiatric imaging data, with autism as an example. Front. Psychiatry 7, 329. http://dx.doi.org/10.3389/fpsyt.2016.00177.
Kelly, C., Toro, R., Di Martino, A., Cox, C.L., Bellec, P., Castellanos, F.X., Milham, M.P., 2012. A convergent functional architecture of the insula emerges across imaging modalities. NeuroImage 61, 1129–1142. http://dx.doi.org/10.1016/j.neuroimage.2012.03.021.
Kohls, G., Schulte-Rüther, M., Nehrkorn, B., Müller, K., Fink, G.R., Kamp-Becker, I., Herpertz-Dahlmann, B., Schultz, R.T., Konrad, K., 2013. Reward system dysfunction in autism spectrum disorders. Social. Cogn. Affect. Neurosci. 8, 565–572. http://dx.doi.org/10.1093/scan/nss033.
Kohls, G., Thönessen, H., Bartley, G.K., Grossheinrich, N., Fink, G.R., Herpertz-Dahlmann, B., Konrad, K., 2014a. Differentiating neural reward responsiveness in autism versus ADHD. Dev. Cogn. Neurosci. 10C, 104–116. http://dx.doi.org/10.1016/j.dcn.2014.08.003.
Kohls, G., Yerys, B.E., Schultz, R.T., 2014b. Striatal development in autism: repetitive behaviors and the reward circuitry. Biol. Psychiatry 76, 358–359. http://dx.doi.org/10.1016/j.biopsych.2014.07.010.
Langen, M., Bos, D., Noordermeer, S.D.S., Nederveen, H., van Engeland, H., Durston, S., 2013. Changes in the development of striatum are involved in repetitive behavior in autism. Biol. Psychiatry. http://dx.doi.org/10.1016/j.biopsych.2013.08.013.
Langen, M., Schnack, H.G., Nederveen, H., Bos, D., Lahuis, B.E., de Jonge, M.V., van Engeland, H., Durston, S., 2009. Changes in the developmental trajectories of striatum in autism. Biol. Psychiatry 66, 327–333. http://dx.doi.org/10.1016/j.biopsych.2009.03.017.
Lawson, R.P., Rees, G., Friston, K.J., 2014. An aberrant precision account of autism. Front. Hum. Neurosci., 8. http://dx.doi.org/10.3389/fnhum.2014.00302.
Lockwood, P.L., 2016. The anatomy of empathy: vicarious experience and disorders of social cognition. Behav. Brain Res. 311, 255–266. http://dx.doi.org/10.1016/j.bbr.2016.05.048.
Lynch, C.J., Uddin, L.Q., Supekar, K., Khouzam, A., Phillips, J., Menon, V., 2013. Default mode network in childhood autism: posteromedial cortex heterogeneity and relationship with social deficits. Biol. Psychiatry 74, 212–219. http://dx.doi.org/10.1016/j.biopsych.2012.12.013.
Mantini, D., Corbetta, M., Romani, G.L., Orban, G.A., Vanduffel, W., 2013. Evolutionarily novel functional networks in the human brain? J. Neurosci. 33, 3259–3275. http://dx.doi.org/10.1523/JNEUROSCI.4392-12.2013.
Mars, R.B., Jbabdi, S., Sallet, J., O'Reilly, J.X., Croxson, P.L., Olivier, E., Noonan, M.P., Bergmann, C., Mitchell, A.S., Baxter, M.G., Behrens, T.E.J., Johansen-Berg, H., Tomassini, V., Miller, K.L., Rushworth, M.F.S., 2011. Diffusion-weighted imaging tractography-based parcellation of the human parietal cortex and comparison with human and macaque resting-state functional connectivity. J. Neurosci. 31, 4087–4100. http://dx.doi.org/10.1523/JNEUROSCI.5102-10.2011.
Mars, R.B., Sallet, J., Schüffelgen, U., Jbabdi, S., Toni, I., Rushworth, M.F.S., 2012. Connectivity-based subdivisions of the human right "temporoparietal junction area": evidence for different areas participating in different cortical networks. Cereb. Cortex 22, 1894–1903. http://dx.doi.org/10.1093/cercor/bhr268.
Mars, R.B., Verhagen, L., Gladwin, T.E., Neubert, F.-X., Sallet, J., Rushworth, M.F.S., 2016. Comparing brains by matching connectivity profiles. Neurosci. Biobehav. Rev. 60, 90–97. http://dx.doi.org/10.1016/j.neubiorev.2015.10.008.
McCann, B.S., 1981. Hemispheric asymmetries and early infantile autism. J. Autism Dev. Disord. 11, 401–411.
Mellet, E., Zago, L., Jobard, G., Crivello, F., Petit, L., Joliot, M., Mazoyer, B., Tzourio-Mazoyer, N., 2014. Weak language lateralization affects both verbal and spatial skills: an fMRI study in 297 subjects. Neuropsychologia 65, 56–62. http://dx.doi.org/10.1016/j.neuropsychologia.2014.10.010.
Mesulam, M.M., Mufson, E.J., 1982. Insula of the old world monkey. III: efferent cortical output and comments on function. J. Comp. Neurol. 212, 38–52. http://dx.doi.org/10.1002/cne.902120104.
Middleton, F.A., Strick, P.L., 2000. Basal ganglia and cerebellar loops: motor and cognitive circuits. Brain Res. Rev. 31, 236–250.
Neubert, F.-X., Mars, R.B., Sallet, J., Rushworth, M.F.S., 2015. Connectivity reveals relationship of brain areas for reward-guided learning and decision making in human and monkey frontal cortex. Proc. Natl. Acad. Sci. 112, E2695–E2704. http://dx.doi.org/10.1073/pnas.1410767112.
Neubert, F.-X., Mars, R.B., Thomas, A.G., Sallet, J., Rushworth, M.F.S., 2014. Comparison of human ventral frontal cortex areas for cognitive control and language with areas in monkey frontal cortex. Neuron 81, 700–713. http://dx.doi.org/10.1016/j.neuron.2013.11.012.
Nyberg, L., Salami, A., Andersson, M., Eriksson, J., Kalpouzos, G., Kauppi, K., Lind, J., Pudas, S., Persson, J., Nilsson, L.-G., 2010. Longitudinal evidence for diminished frontal cortex function in aging. Proc. Natl. Acad. Sci. 107, 22682–22686. http://dx.doi.org/10.1073/pnas.1012651108.
Padmanabhan, A., Lynn, A., Foran, W., Luna, B., O'Hearn, K., 2013. Age related changes in striatal resting state functional connectivity in autism. Front. Hum. Neurosci. 7, 814. http://dx.doi.org/10.3389/fnhum.2013.00814.
Patel, A.X., Kundu, P., Rubinov, M., Jones, P.S., Vértes, P.E., Ersche, K.D., Suckling, J., Bullmore, E.T., 2014. A wavelet method for modeling and despiking motion artifacts from resting-state fMRI time series. NeuroImage 95, 287–304. http://dx.doi.org/10.1016/j.neuroimage.2014.03.012.
Pauli, W.M., O'Reilly, R.C., Yarkoni, T., Wager, T.D., 2016. Regional specialization within the human striatum for diverse psychological functions. Proc. Natl. Acad. Sci. 113, 1907–1912. http://dx.doi.org/10.1073/pnas.1507610113.
Pellicano, E., Burr, D., 2012. When the world becomes "too real": a Bayesian explanation of autistic perception. Trends Cogn. Sci. 16, 504–510. http://dx.doi.org/10.1016/j.tics.2012.08.009.
Picci, G., Scherf, K.S., 2015. A two-hit model of autism: adolescence as the second hit. Clin. Psychol. Sci. 3, 349–371. http://dx.doi.org/10.1177/2167702614540646.
Power, J.D., Barnes, K.A., Snyder, A.Z., Schlaggar, B.L., Petersen, S.E., 2012. Spurious but systematic correlations in functional connectivity MRI networks arise from subject motion. NeuroImage 59, 2142–2154. http://dx.doi.org/10.1016/j.neuroimage.2011.10.018.
Price, C.J., 2010. The anatomy of language: a review of 100 fMRI studies published in 2009. Ann. New Y. Acad. Sci. 1191, 62–88. http://dx.doi.org/10.1111/j.1749-6632.2010.05444.x.
Pruim, R.H.R., Mennes, M., Buitelaar, J.K., Beckmann, C.F., 2015a. Evaluation of ICA-AROMA and alternative strategies for motion artifact removal in resting state fMRI. NeuroImage 112, 278–287. http://dx.doi.org/10.1016/j.neuroimage.2015.02.063.
Pruim, R.H.R., Mennes, M., van Rooij, D., Llera, A., Buitelaar, J.K., Beckmann, C.F., 2015b. ICA-AROMA: a robust ICA-based strategy for removing motion artifacts from fMRI data. NeuroImage 112, 267–277. http://dx.doi.org/10.1016/j.neuroimage.2015.02.064.
Rademacher, L., Krach, S., Kohls, G., Irmak, A., Grunder, G., 2010. Dissociation of neural networks for anticipation and consumption of monetary and social rewards. NeuroImage.
Radulescu, E., Ganeshan, B., Minati, L., Beacher, F.D.C.C., Gray, M.A., Chatwin, C., Young, R.C.D., Harrison, N.A., Critchley, H.D., 2013a. Gray matter textural heterogeneity as a potential in-vivo biomarker of fine structural abnormalities in Asperger syndrome. Pharmacogenomics J. 13, 70–79. http://dx.doi.org/10.1038/tpj.2012.3.
Radulescu, E., Minati, L., Ganeshan, B., Harrison, N.A., Gray, M.A., Beacher, F.D.C.C., Chatwin, C., Young, R.C.D., Critchley, H.D., 2013b. Abnormalities in fronto-striatal connectivity within language networks relate to differences in grey-matter heterogeneity in Asperger syndrome. NeuroImage: Clin. 2, 716–726. http://dx.doi.org/10.1016/j.nicl.2013.05.010.
Richey, J.A., Rittenberg, A., Hughes, L., Damiano, C.R., Sabatino, A., Miller, S., Hanna, E., Bodfish, J.W., Dichter, G.S., 2014. Common and distinct neural features of social and non-social reward processing in autism and social anxiety disorder. Social. Cogn. Affect. Neurosci. 9, 367–377. http://dx.doi.org/10.1093/scan/nss146.
Rinehart, N.J., Bradshaw, J.L., Brereton, A.V., 2002. Lateralization in individuals with high-functioning autism and Asperger's disorder: a frontostriatal model. J. Autism. http://dx.doi.org/10.1023/A:1016387020095.
Robinson, J.L., Laird, A.R., Glahn, D.C., Blangero, J., Sanghera, M.K., Pessoa, L., Fox, P.M., Uecker, A., Friehs, G., Young, K.A., Griffin, J.L., Lovallo, W.R., Fox, P.T., 2012. The functional connectivity of the human caudate: an application of meta-analytic connectivity modeling with behavioral filtering. NeuroImage 60, 117–129. http://dx.doi.org/10.1016/j.neuroimage.2011.12.010.
Rousseeuw, P.J., 1987. Silhouettes: a graphical aid to the interpretation and validation of cluster analysis. J. Comput. Appl. Math. 20, 53–65. http://dx.doi.org/10.1016/0377-0427(87)90125-7.
Ryali, S., Chen, T., Supekar, K., Menon, V., 2013. A parcellation scheme based on von Mises-Fisher distributions and Markov random fields for segmenting brain regions using resting-state fMRI. NeuroImage 65, 83–96. http://dx.doi.org/10.1016/j.neuroimage.2012.09.067.
Sallet, J., Mars, R.B., Noonan, M.P., Neubert, F.X., Jbabdi, S., O'Reilly, J.X., Filippini, N., Thomas, A.G., Rushworth, M.F., 2013. The organization of dorsal frontal cortex in humans and macaques. J. Neurosci. 33, 12255–12274. http://dx.doi.org/10.1523/JNEUROSCI.5108-12.2013.
Satterthwaite, T.D., Elliott, M.A., Gerraty, R.T., Ruparel, K., Loughead, J., Calkins, M.E., Eickhoff, S.B., Hakonarson, H., Gur, R.C., Gur, R.E., Wolf, D.H., 2013. An improved framework for confound regression and filtering for control of motion artifact in the preprocessing of resting-state functional connectivity data. NeuroImage 64, 240–256 . http://dx.doi.org/10.1016/j.neuroimage.2012.08.052.
Schmitz, N., Rubia, K., Daly, E., Smith, A., Williams, S., Murphy, D.G.M., 2006. Neural correlates of executive function in autistic spectrum disorders. BPS 59, 7–16. http://dx.doi.org/10.1016/j.biopsych.2005.06.007.
Schuetze, M., Park, M.T.M., Cho, I.Y., MacMaster, F.P., Chakravarty, M.M., Bray, S.L., 2016. Morphological alterations in the thalamus, striatum, and pallidum in autism spectrum disorder. Neuropsychopharmacology 41, 2627–2637. http://dx.doi.org/10.1038/npp.2016.64.
Scott-Van Zeeland, A.A., Dapretto, M., Ghahremani, D.G., Poldrack, R.A., Bookheimer, S.Y., 2010a. Reward processing in autism. Autism Res. 3, 53–67. http://dx.doi.org/10.1002/aur.122.
Scott-Van Zeeland, A.A., McNealy, K., Wang, A.T., Sigman, M., Bookheimer, S.Y., Dapretto, M., 2010b. No neural evidence of statistical learning during exposure to artificial languages in children with autism spectrum disorders. Biol. Psychiatry 68, 345–351. http://dx.doi.org/10.1016/j.biopsych.2010.01.011.
Selemon, L.D., Goldman Rakic, P.S., 1985. Longitudinal topography and interdigitation of corticostriatal projections in the rhesus monkey. J. Neurosci. 5, 776–794.
Shen, X., Papademetris, X., Constable, R.T., 2010. Graph-theory based parcellation of

functional subunits in the brain from resting-state fMRI data. NeuroImage 50, 1027–1035. http://dx.doi.org/10.1016/j.neuroimage.2009.12.119.
Shen, X., Tokoglu, F., Papademetris, X., Constable, R.T., 2013. Groupwise whole-brain parcellation from resting-state fMRI data for network node identification. NeuroImage 82, 403–415. http://dx.doi.org/10.1016/j.neuroimage.2013.05.081.
Takarae, Y., Minshew, N.J., Luna, B., Sweeney, J.A., 2007. Atypical involvement of frontostriatal systems during sensorimotor control in autism. Psychiatry Res. 156, 117–127. http://dx.doi.org/10.1016/j.pscychresns.2007.03.008.
Tyszka, J.M., Kennedy, D.P., Paul, L.K., Adolphs, R., 2014. Largely typical patterns of resting-state functional connectivity in high-functioning adults with autism. Cereb. Cortex 24, 1894–1905. http://dx.doi.org/10.1093/cercor/bht040.
Tziortzi, A.C., Haber, S.N., Searle, G.E., Tsoumpas, C., Long, C.J., Shotbolt, P., Douaud, G., Jbabdi, S., Behrens, T.E.J., Rabiner, E.A., Jenkinson, M., Gunn, R.N., 2014. Connectivity-based functional analysis of dopamine release in the striatum using diffusion-weighted MRI and positron emission tomography. Cereb. Cortex 24, 1165–1177. http://dx.doi.org/10.1093/cercor/bhs397.
Uddin, L.Q., Kelly, A.M., Biswal, B.B., Castellanos, F.X., Milham, M.P., 2009. Functional connectivity of default mode network components: correlation, anticorrelation, and causality. Hum. Brain Mapp. 30, 625–637. http://dx.doi.org/10.1002/hbm.20531.
Uddin, L.Q., Menon, V., 2009. The anterior insula in autism: under-connected and under-examined. Neurosci. Biobehav. Rev..
Uddin, L.Q., Menon, V., Young, C.B., Ryali, S., Chen, T., Khouzam, A., Minshew, N.J., Hardan, A.Y., 2011. Multivariate searchlight classification of structural magnetic resonance imaging in children and adolescents with autism. Biol. Psychiatry 70, 833–841. http://dx.doi.org/10.1016/j.biopsych.2011.07.014.
Uddin, L.Q., Supekar, K., Menon, V., 2013. Reconceptualizing functional brain connectivity in autism from a developmental perspective. Front. Hum. Neurosci. 7, 458. http://dx.doi.org/10.3389/fnhum.2013.00458.
Van de Cruys, S., Evers, K., Van der Hallen, R., Van Eylen, L., Boets, B., de-Wit, L., Wagemans, J., 2014. Precise minds in uncertain worlds: predictive coding in autism. Psychol. Rev. 121, 649–675. http://dx.doi.org/10.1037/a0037665.
Verstynen, T.D., Badre, D., Jarbo, K., Schneider, W., 2012. Microstructural organizational patterns in the human corticostriatal system. J. Neurophysiol. 107, 2984–2995. http://dx.doi.org/10.1152/jn.00995.2011.
Volman, I., Roelofs, K., Koch, S., Verhagen, L., Toni, I., 2011a. Anterior prefrontal cortex inhibition impairs control over social emotional actions. Curr. Biol. 21, 1766–1770. http://dx.doi.org/10.1016/j.cub.2011.08.050.
Volman, I., Toni, I., Verhagen, L., Roelofs, K., 2011b. Endogenous testosterone modulates prefrontal-amygdala connectivity during social emotional behavior. Cereb. Cortex 21, 2282–2290. http://dx.doi.org/10.1093/cercor/bhr001.
Wig, G.S., Laumann, T.O., Petersen, S.E., 2014. An approach for parcellating human cortical areas using resting-state correlations. NeuroImage 93 (Pt 2), 276–291. http://dx.doi.org/10.1016/j.neuroimage.2013.07.035.
Wilke, M., Holland, S.K., Altaye, M., Gaser, C., 2008. Template-O-Matic: a toolbox for creating customized pediatric templates. NeuroImage 41, 903–913. http://dx.doi.org/10.1016/j.neuroimage.2008.02.056.
Winkler, A.M., Ridgway, G.R., Webster, M.A., Smith, S.M., Nichols, T.E., 2014. Permutation inference for the general linear model. NeuroImage 92, 381–397. http://dx.doi.org/10.1016/j.neuroimage.2014.01.060.
Woo, C.-W., Krishnan, A., Wager, T.D., 2014. Cluster-extent based thresholding in fMRI analyses: pitfalls and recommendations. NeuroImage 91, 412–419. http://dx.doi.org/10.1016/j.neuroimage.2013.12.058.
Yan, C.-G., Cheung, B., Kelly, C., Colcombe, S., Craddock, R.C., Di Martino, A., Li, Q., Zuo, X.-N., Castellanos, F.X., Milham, M.P., 2013. A comprehensive assessment of regional variation in the impact of head micromovements on functional connectomics. NeuroImage 76, 183–201. http://dx.doi.org/10.1016/j.neuroimage.2013.03.004.
Yeo, B.T.T., Krienen, F.M., Sepulcre, J., Sabuncu, M.R., Lashkari, D., Hollinshead, M., Roffman, J.L., Smoller, J.W., Zöllei, L., Polimeni, J.R., Fischl, B., Liu, H., Buckner, R.L., 2011. The organization of the human cerebral cortex estimated by intrinsic functional connectivity. J. Neurophysiol. 106, 1125–1165. http://dx.doi.org/10.1152/jn.00338.2011.
Yeterian, E.H., Pandya, D.N., 1991. Prefrontostriatal connections in relation to cortical architectonic organization in rhesus monkeys. J. Comp. Neurol. 312, 43–67. http://dx.doi.org/10.1002/cne.903120105.